Heritage Science

RESEARCH

Open Access

Development of a methodology for the characterisation and assessment of biodeteriogens on archaeological surfaces by use of a portable LED-induced fluorescence instrument

A. Giakoumaki[1*], A. Philippidis[1], P. Siozos[1], I. Pyrri[2], D. Anglos[1,3] and P. Pouli[1]

Abstract

The present study focuses on the development of a fast, non-invasive methodology, appropriate for the detection and characterization of biodeterioration present on the surface of archaeological/historical stone objects and monuments, by exploiting the characteristic fluorescence emission of biological deposits. Fluorescence spectra were collected by use of a portable LED (Light Emitting Diode)-Induced Fluorescence (LED-IF) instrument. Three limestone fragments and one mortar fragment, from different monuments in Greece, presenting various types of biodeterioration on their surface, have been investigated in the laboratory. First, fluorescence emission spectra were acquired with a benchtop laboratory spectrofluorometer in order to select the optimum excitation wavelengths for the fluorophores present in the biological crust. An evaluation of the portable LED-IF instrument was conducted by assessing the performance of its optical components and different LED excitation sources, while an investigation of several experimental parameters on the fluorescence signal was also performed. Furthermore, issues related to the efficiency of detection and identification of biological growth have been studied, such as the effect of sample surface wetting on the fluorescence signal. The results of the present study demonstrate that the LED-IF instrument can be used for a fast and reliable assessment of the presence of biodeterioration on monuments.

Keywords: Stone monuments, Biodeterioration, LED-induced fluorescence, Portable instrumentation

Introduction

Biological deterioration is one of the main decline factors of the physical, chemical and mechanical properties of materials on historical buildings as well as of the overall aesthetic appearance of monuments. Building walls and monument surfaces might suffer many different types of biological deterioration, even on adjacent areas, depending on their specific location on the monument and their orientation, which relate to different sunlight exposure, temperature, rainfall profile, or wind and humidity conditions among others. Also, surface morphology and sculpturing details, as well as composition and microstructure of the materials may influence both the type and growth of biodeteriogens. The different types of microorganisms/organisms that can colonise a historic building include cyanobacteria, algae, moss (photoautotrophic organisms), fungi (heterotrophic organisms), lichens (a symbiotic partnership between algae/cyanobacteria and fungi) and bacteria among others [1–6].

*Correspondence: agiakoumaki@iesl.forth.gr

[1] Institute of Electronic Structure and Laser, Foundation for Research and Technology-Hellas (IESL-FORTH), 100 N. Plastira St., 70013 Heraklion, Crete, Greece
Full list of author information is available at the end of the article

These microorganisms, in many cases, need to be removed. However, as regards certain types of biodeteriogens their removal may sometimes be not only needless, but can also be even more disruptive than their mere presence on the monument [2]. Therefore, the characterisation of biological deterioration is an essential first step that can help conservators, heritage scientists and archaeologists to make informed decisions on their further actions and management of a monument.

The most common microbiological and molecular techniques for the characterisation of microbial colonisation on stone monuments include isolation and culture of microorganisms on artificial nutrient media, enzyme-linked immunosorbent assay, fluorescence microscopy, nucleic acids isolation, Polymerase Chain Reaction (PCR), hybridization (e.g. FISH—Fluorescent In-Situ Hybridization), classical or high throughput sequencing [7, 8]. Various microscopies, electron- or photon-based, are also used, such as Scanning Electron Microscopy (SEM) and wet-mode Environmental SEM, Transmission Electron Microscopy (TEM), confocal laser scanning microscopy with CTC (tetrazolium salt 5-cyano-2,3-ditolyltetrazolium chloride) staining and epifluorescence microscopy [7, 8]. Furthermore, methods for detecting the stone pigmentation changes include chlorophyll content determination and total colour difference [7, 8]. All these techniques require sampling, which can introduce errors in terms of obtaining a representative assessment of the biodeterioration. Additionally, it needs to be decided whether the removal of a representative sample and the damage that may be incurred as a result of this sampling, counterbalances the information gained. Furthermore, sampling includes scraping off material from the stone surface, cutting etc., which in many cases can be prohibitive due to the value of the monument. Finally, sample preparation, essential in many techniques, is generally costly and time-consuming.

Therefore, the application of an easy-to-use, non-invasive analytical method with the purpose to characterise and classify in-situ the different types of biological deterioration, avoiding sampling and sample preparation altogether, would decrease analysis time, leading faster to a timely and efficient treatment of the biodeterioration. Fluorescence is a technique that meets all the previously mentioned requirements and has been successfully used for monitoring and characterisation of photoautotrophic biodeterioration on monuments [2].

The substances in biodeteriogens that fluoresce are mainly pigments and other compounds such as ferulic acids, phenyl-propanoids etc. Three main classes of pigments are employed by oxygenic organisms for harvesting sunlight: chlorophylls, phycobilins (phycoerythrin, phycocyanin and allophycocyanin) and carotenoids. Chlorophylls and phycobilins have large absorption cross-sections and fluoresce easily; quantum yields for chlorophyll species are in the range of 0.1–0.25 [9], while for allophycocyanin the quantum yield is 0.4 [10]. Carotenoids absorb light efficiently between 450 and 550 nm but have very low fluorescence yields (the fluorescence quantum yield of β-carotene has been reported to be 1×10^{-4}) [11].

The main pigment that is present in all photoautotrophic organisms is chlorophyll a (Photosystem II-PSII) and exhibits a typical fluorescence band at 685 nm [12–15]. Furthermore, a fluorescence emission band at 720–740 nm appears in leaves of higher plants, which is mainly associated with Photosystem I (PSI) but is also related with vibronic emissions of chlorophyll species associated with PSII [12, 14]. There exist also other types of chlorophyll, namely chlorophyll *b* with fluorescence emission maxima at 650–660 nm, as well as chlorophylls *c* and *d* [12, 14, 16].

As regards phycobilins, there exist several types, such as phycoerythrin, phycocyanin and allophycocyanin, whose fluorescence emission profiles center at 640–660 nm, 645–655 nm and 660–675 nm, respectively [14, 17]. Other substances related to biodeteriogens that could fluoresce are nicotinamide adenine dinucleotide (NADH) and riboflavin with maxima at 490 nm and 525 nm respectively [18].

In Table 1, relevant optical properties, namely absorption (λ_{abs}) and fluorescence emission (λ_{em}) band maxima of chromophores that could be found in common biodeteriogens are summarised. It is noted that the data reported in Table 1 correspond mostly to measurements in solutions of the chromophores.

In situ fluorescence analysis of monument surfaces has been performed by use of Laser Induced Fluorescence-Light Detection and Ranging (LIF-LIDAR) and results have been reported in the literature. For example, researchers from Italy have managed to record fluorescence spectra using a LIDAR system for the analysis of the façade of the Parma cathedral and baptistery (Italy) [30]. In addition, the same group was able to differentiate between cyanobacteria and green algae using a laboratory setup with the same components that can be employed in a LIDAR system [31]. A research team from Sweden scanned the façade of the Parma Cathedral recording the fluorescence signal with a LIDAR setup [32]. Furthermore, a collaboration between the Swedish and Italian teams led to successful mapping of the façade of the Lund Cathedral (Sweden) and acquiring fluorescence spectral signatures from various building materials as well as the biodeterioration colonisation (green algae and lichens) recording primarily the band of chlorophyll at 680 nm [33]. The same two groups

Table 1 Typical biodeteriogens/microbial groups encountered in monuments with absorption and fluorescence emission properties of key chromophores. λ_{abs} and λ_{em} refer to wavelengths reported in the literature cited

Microbial groups	Compound	λ_{abs} (nm)	References	λ_{em} (nm)	References
Algae/moss (photoautotroph)	Chlorophyll *a*	405, 418, 670	[19, 20]	685, 720, 735	[12, 13]
	Chlorophyll *b*	413, 450	[19, 21]	650–660	[13, 16]
Cyanobacteria* (photoautotroph)	Phycocyanin	580, 625, 634–637	[17]	645–653	[14, 17]
	Phycoerythrin	570		580, 640–660	
	Allophycocyanin	650		660–675	
Fungi (heterotroph)	Melanin	330	[18, 22]	440, 520, 540, 575	[18, 23]
	Riboflavin	371, 442	[24]	525–535	[18, 24]
	NADH	290–295, 340	[18, 23]	493, 450–475	[18, 23, 25]
	Chitin	330	[26]	413, 440, 452–458	[23, 26]
	Tryptophan	240, 290, 340	[27]	330–340, 340–353, 363	[23, 28, 29]
	Tyrosine	260		300–310	

* In cyanobacteria, chlorophyll *a* and *b* can also be present

performed hyperspectral fluorescence imaging with two LIDAR systems on the Colosseum (Italy) in order to visualise and map past conservation interventions [34]. The fluorescence LIDAR technique in the context of cultural heritage applications has been reviewed in a book chapter and a publication [15, 35].

In the aforementioned LIDAR systems, the excitation source is a pulsed laser. The use of a powerful pulsed laser for outdoors measurements entails certain limitations. Generally, these lasers are costly and bulky and in addition safety considerations must be taken into account. Therefore, the use of a continuous light source would be preferred for outdoors applications and indeed in the past few years, continuous laser sources in LIDAR setups have been reported. Fluorescence measurements were conducted on vegetation [36], as well as oil spills on river water [37]. In the past decade, the use of LEDs as excitation sources is gaining ground on a wide range of fluorescence measurements [38]. Several applications of LED-Induced Fluorescence (LED-IF) have been reported, including tea classification and quality assessment [39], detection of various types of foreign matter in cotton, of both botanical and non-botanical origin [40], monitoring of apple freshness and quality [41], or milk freshness [42] and determination of sulphur content in diesel/biodiesel blends [43] among others. Recently, a portable spectrofluorometer (LEDμSF) using a LED source for excitation was developed for the in-situ analysis of pigments and binders in fragile artworks [44]. However, to the authors' knowledge, the LED-IF technique has not been applied so far for in-situ measurements of biodeterioration on materials of archaeological and historic interest.

The present study has outlined a versatile methodology for the reliable characterization and assessment of biodeterioration on monuments by means of a newly-developed portable LED-IF spectrometer. Instrumentation aspects, including selection of the proper LED emission wavelength and fluorescence measurement optimization, as well as methodological ones, for example, treatment (wetting) of samples have been investigated leading to the successful detection and characterisation of different types of biodeterioration. This portable LED-IF spectrometer can be proved a powerful tool at the hands of conservators, archaeologists and other scientists, who can quickly and easily evaluate the state of biodeterioration at historical buildings or archaeological monuments and take proper actions towards their conservation.

Experimental setup—materials and methods

Objects studied

Four objects exhibiting biological decay were investigated, all collected from different archaeological sites in Greece. Three of them are limestone fragments (objects A, B and C) and one is a mortar fragment (object D). Object A is a soft limestone from Peloponnese, object B is a grey limestone from Epirus, object C is a limestone from Peloponnese and object D is a mortar from the island of Zakynthos (Zante). A leaf from a *Hibiscus* plant was also examined, in order to obtain a reference spectrum for chlorophyll species, expected to be present in some biodeteriogens.

The objects have been photographed with an SLR digital camera (EOS 760D, Canon, Lens EF-S 18–55 mm) and the area analyzed on each one is marked by a red circle on the corresponding image (Fig. 1, left column; in the inset the whole object can be seen). For a more detailed view of the analysis area, images were acquired (Fig. 1, middle column) by means of a digital microscope (Dino-Lite, The Netherlands—magnification: × 45–50).

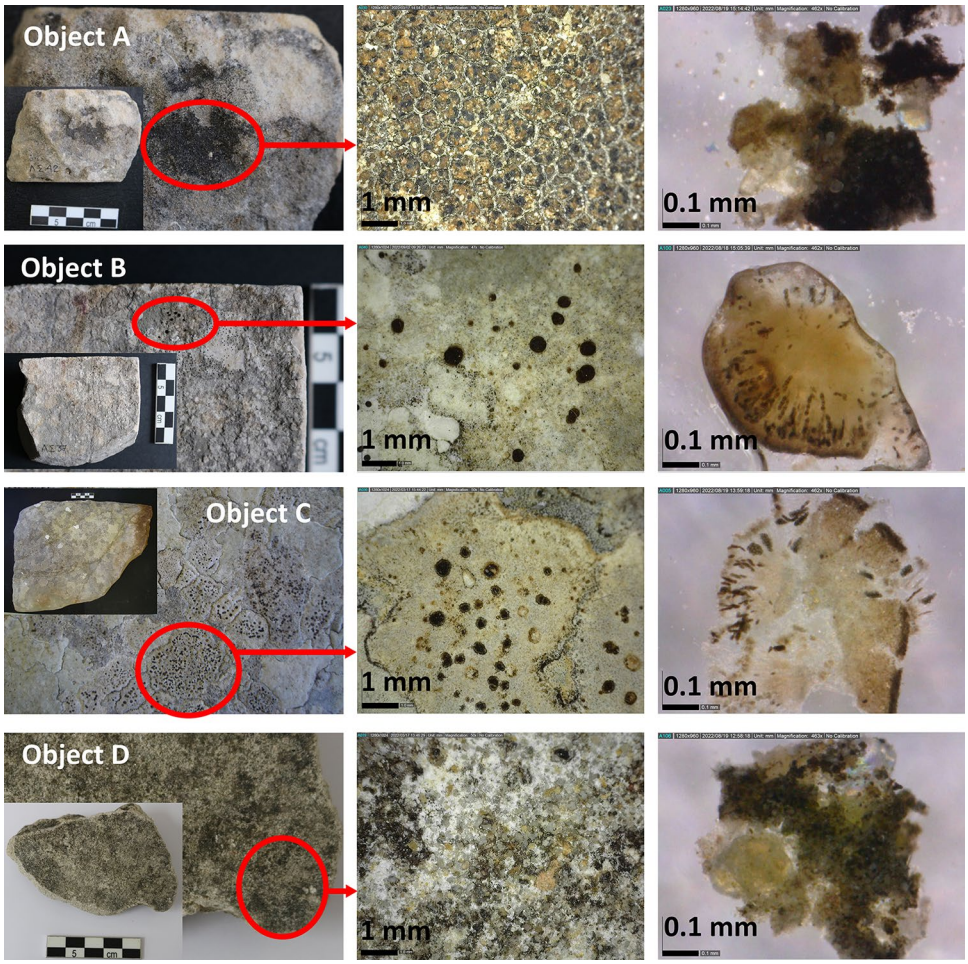

Fig. 1 Images of the archaeological objects investigated, with the area analysed on the surface of each one, indicated by a red circle (left column; inset: the whole object is shown). The analysis area was photographed also with a magnification × 45–50 (middle column). Images of the samples prepared for performing the classical taxonomy analysis (right column; magnification: × 460)

In order to verify the presence and assess the type of biodeteriogens on the items studied, a classical identification based on optical microscopy was undertaken by an expert biologist. Less than 1 mg of material was scraped off the object's surface with a needle and transferred onto a microscope slide. The material was mounted with a drop of deionised water and covered with a cover slip. The biological material was observed under a digital microscope (Dino-Lite, magnification: × 460) (Fig. 1, right column).

All objects were wetted prior to fluorescence analysis and the reasons that led us to adopt this approach are explained in "The effect of wetting the samples surface on the fluorescence signal" Section. The samples were sprayed with distilled water each time before analysis so as to create a thin water film on the area probed and measurements were obtained a few minutes following wetting. The amount of water was equivalent to about 0.2 ml (one spray shot) spread over a surface area of about 5×5 cm^2, thus corresponding to 8×10^{-3} ml/cm^2. Distilled water was chosen against tap water so that no extra minerals/impurities contained in tap water would be added to the objects under examination.

Instrumentation

Fluorescence emission measurements on the objects were carried out by use of a hybrid-portable spectrometer (LMNTII+) [45] originally developed for performing combined LIBS (elemental analysis) and diffuse reflectance measurements. In the context of the current study, the instrument was appropriately modified so as to accommodate LED-IF measurements. This was achieved by replacing the tungsten-halogen lamp (used for the diffuse reflectance measurements) with a LED excitation source.

In the present series of LED-IF experiments, two LED sources, emitting at 375 nm (M375L4, Thorlabs, USA) and 440 nm (M455L3, Thorlabs, USA) respectively, were evaluated. An aspheric condenser lens with a focal distance of f = + 20 mm focusses the LED irradiation on the sample down to a spot size of about 2×2 mm^2. The maximum power (P) of each LED reaching the sample, with both a band-pass filter (see "Evaluation of instrument performance and measurement parameters" Section for details on the filters) and the focusing lens in the LED's light path, was measured with a FieldMate power meter (Coherent, USA) and was P = 6 mW and P = 26 mW for the LED emitting at 375 nm and 440 nm respectively.

The emitted fluorescence was collected by use of a simple optical telescope (two convergent lenses with focal distances of $f_1 = +75$ mm and $f_2 = +25$ mm) and introduced into a 200 μm diameter optical fibre, coupled, on its other end, to the entrance slit of the spectrometer, an AvaSpec-ULS2048CL-EVO (Avantes, Netherlands) operated through a laptop computer via the AvaSoft 8 software. The spectrum coverage is in the range of 200–1100 nm and the spectral resolution is 2.5 nm (entrance slit width = 50 μm, diffraction grating: 300 lines/mm). The emission signal integration time used for the LED-IF measurements was 300 ms.

Additionally, a FluoroMax-P laboratory spectrofluorometer (Horiba/Jobin Yvon) using a cw Xenon arc lamp as excitation source, was employed for preliminary analysis of the objects studied. Fluorescence spectra were acquired, by placing the samples at approximately 45° with respect to the incident excitation beam, supplied by the excitation monochromator, and emission was collected at 90°, with respect to the incident beam, into the emission monochromator. Typical integration time was 0.5–1 s/nm.

Results and discussion

The first step of our study was to acquire basic biological data regarding the taxonomic status of the main microbial colonizers of the biofilms. Following preparation, samples were examined, by one of the authors (IP), under a digital microscope (magnification: × 460) and the main microbial groups were identified. For objects B and C, the biological material was sampled from the areas indicated by the dark-coloured spots observed in Fig. 1 (middle column) and the presence of lichens was revealed. For objects A and D, the biological material was scraped off the surface of the samples (Fig. 1, middle column) and the main colonizers were found to be algae (green areas) and fungi (black or brown areas). This information was essential in order to properly validate the results of our fluorescence spectroscopic analysis.

The next step involved the evaluation of the operational and performance characteristics of the LED-IF-adapted portable spectrometer (LED, filters, optics, spectrometer-detector) as well as the development of a straightforward measurement methodology that are essential prerequisites for the design of an instrument, which will ensure acquisition of reproducible and reliable results both in the laboratory and in the field. The aspects investigated include among others: (a) evaluation of the optical components of the instrument, (b) selection of the proper LED source, (c) comparison of fluorescence spectra acquired with the portable system against those obtained by use of a conventional laboratory fluorometer (d) study of the signal evolution (stability) over time, (e) treatment of the samples. In the following sections, the above aspects are detailed and the results of our studies are presented and discussed.

Evaluation of instrument performance and measurement parameters

Given that excitation is a critical experimental parameter when performing fluorescence measurements, we focussed our attention on the emission characteristics of the LED sources in terms of both spectral output and emission intensity. As widely known, LEDs emit light with a considerably broader spectral bandwidth compared to lasers and even to laboratory fluorometers, which make use of an excitation monochromator to select a narrow band from the output of a high intensity Xe arc lamp. The wide emission peak of the LED could on the one hand compromise selectivity in the excitation and, on the other, mask or superimpose on possible fluorescence features appearing in the vicinity of the LED excitation wavelength range. Given that fluorescence emission measurements require excitation at a relatively narrow spectral bandwidth, typically 1–5 nm, we employed narrow band-pass filters to reduce the FWHM of the LED spectral output. To this end, a band-pass filter at 370 nm (FB370-10, Thorlabs, USA, FWHM = 10 nm) was placed in front of the LED emitting at 375 nm and likewise a laser line filter at 441.6 nm (FL441.6-10, Thorlabs, USA, FWHM = 10 nm) was used for the LED emitting at 440 nm. In Fig. 2, the emission spectra of the LED sources are shown both raw and following transmission through the band-pass filters used. In order to measure the emission FWHM, a relatively low LED power has been employed so that the LED intensity does not lead the detector to saturation. It was found that, by use of the filters, the FWHM is reduced from 15 nm down to 10 nm for the visible LED (440 nm) and, likewise, from 11 nm down to 6 nm for the ultraviolet LED source (375 nm). It is noted that during fluorescence measurements, the

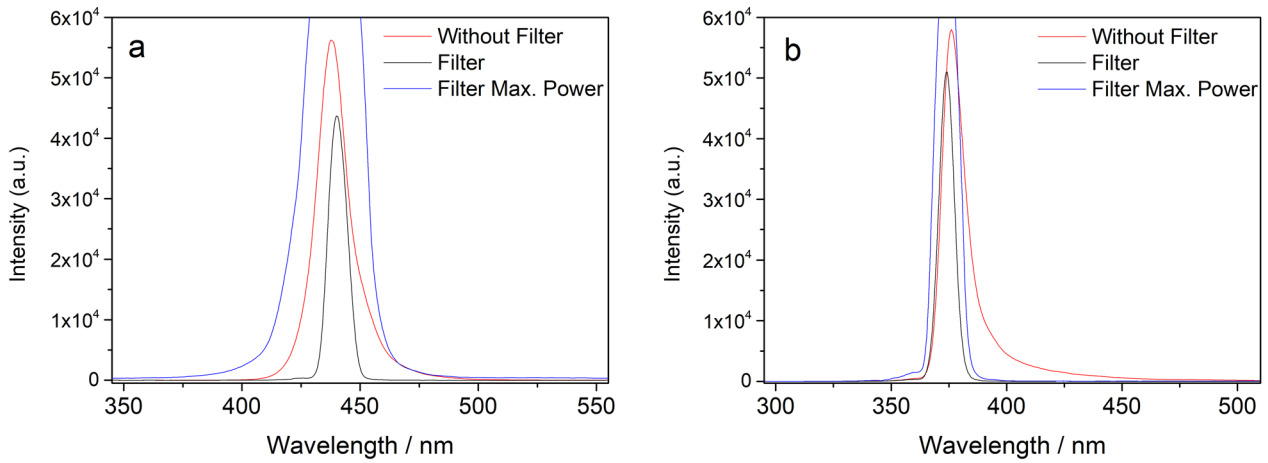

Fig. 2 Emission spectra of the two LED sources emitting at $\lambda_{exc} = 440$ nm (**a**) and $\lambda_{exc} = 375$ nm (**b**), with (black) and without (red) a band-pass interference filter in the beam path. Spectra are also shown (blue) corresponding to the maximum output power for each LED source, also acquired in the presence of the band pass filter

maximum available power of the LED is applied and thus one should be aware that non-negligible excitation is supplied even at the wings of the spectral profile.

Apart from narrowing down the FWHM, the use of filters resulted in shifts, in the emission maximum of the LED spectral output mainly because of the mismatch between the bandpass filter's transmission maximum and the LED emission maximum. The ultraviolet LED shifted down to 374 nm (bandpass filter central wavelength: 370 nm), while the blue LED showed an up-shift to 440 nm (filter's central wavelength: 441.6 nm). These features, although not crucial for our measurements, need to be known prior to analysis for a complete characterisation of the portable system.

Regarding the fluorescence signal acquisition, it is of concern the fact that the increased integration time applied (i.e. 300 ms), may lead to significant interference from ambient light. To avoid this complexity, spectra need to be acquired in the dark, which in many cases is difficult if not impossible, particularly when measurements are acquired outdoors. This problem is addressed by means of spectral background correction, a feature available by the spectrometer software. Figure 3 shows raw background spectra (LED off, no sample) acquired with the laboratory lights on (black line) and defined as "dark" in the spectrometer software. Then background-corrected spectra (red line) were acquired with the spectrometer operated at the "scope corrected for dark" mode (i.e. spectrum displayed after subtracting the "dark" spectrum), with the ambient light peaks successfully eliminated.

To further verify the applicability of the background subtraction feature, test measurements were conducted

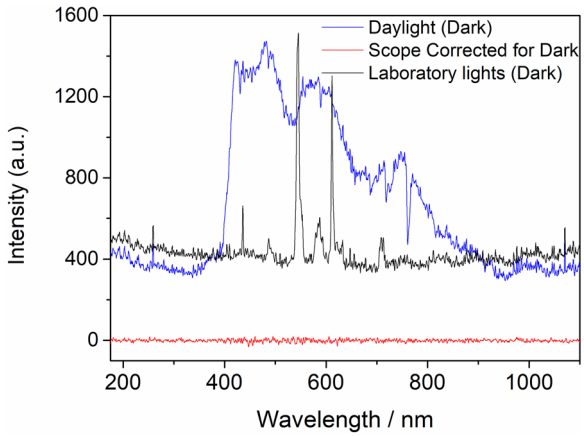

Fig. 3 "Dark" spectrum acquired on the LED-IF instrument with laboratory lights on (black), in daylight (blue) and background corrected spectrum, "scope corrected for dark" (red)

outdoors, in daylight conditions, and following acquisition of a "dark" spectrum (Fig. 3, blue line) it was confirmed that upon background subtraction the resulting "scope corrected for dark" spectrum was also free of any interference. This background subtraction feature is indeed convenient, if long integration times need to be used, especially when measurements are performed in-situ (archaeological/historical sites and monuments).

Following initial observations that evidenced changes with time of the fluorescence emission signals, collected from the biological encrustation, we decided to investigate the stability of the fluorescence emission signal over time. For this reason, a set of 10 consecutive LED-IF

measurements (each corresponding to integration time of 300 ms, LED emitting at 440 nm) was carried out on the same spot of a *Hibiscus* leaf sample (Fig. 4a). The two bands at 685 and 735 nm are assigned to chlorophyll species (Chl) (see Table 1 and Introduction for further explanations) and it is quite evident that, with continuous excitation by the LED beam, the overall emission intensity drops, while also the relative intensity of the bands changes. By integrating the area under the two bands, one observes that the total fluorescence emission intensity decreases abruptly, until half-way in the spectral series and eventually approaches a rather stable regime (Fig. 4b). This observation can be interpreted either on the basis of chromophore photobleaching [46] or as a result of chlorophyll fluorescence quenching. The latter has been previously observed by Kautsky [47]; upon transferring photosynthetic material from darkness to light an increase in the chlorophyll fluorescence occurs over a time period of 1 s and then following this, the fluorescence intensity level typically starts falling again over a time scale of a few minutes, depending on the species [47].

Given that comparisons among different areas bearing biodeterioration are to be made, which might help one to estimate the quantity of the biological deposit, it is important to conduct measurements under conditions which warrant signal stability. As observed in Fig. 4b any measurement performed in the stabilised intensity regime can be considered as acceptable and, in the context of the present study, it was decided to keep the spectrum from the 10th measurement and this was consistently followed throughout the experiments.

Fluorescence characteristics of biodeteriogens

In the beginning of this study, a preliminary set of fluorescence measurements was conducted on the stone objects, utilizing the Fluoromax benchtop spectrofluorometer. This facilitated a better understanding of the fluorescence emission properties of the biological deposits investigated and moreover indicated the excitation wavelength range most suitable for obtaining efficient excitation of the chromophores and thus securing optimum detection of their fluorescence emission. These measurements also provided critical input needed in order to select the most suitable LED for the portable instrument and, in addition, served as a reference against which to compare the LED-IF data.

Fluorescence emission spectra were recorded upon excitation at wavelengths varying from 400 to 600 nm in increments of 25 nm (excitation wavelength scanning). The two limestone objects (A and B), the mortar object (D) and the *Hibiscus* leaf were studied. The archaeological samples were introduced in the sample chamber following wetting of their surface according to the procedure described in "Experimental setup—materials and methods" Section (see also "The effect of wetting the samples surface on the fluorescence signal" Section). The third limestone object, C, was not analysed because its large size made it impossible to position it properly in the sample chamber of the fluorometer. To ensure reproducibility, the excitation wavelength scanning was carried out three times for each sample at the same area (marked by a red circle in the images shown in Fig. 1). The reported spectra represent the average of the three different acquisitions. In the case of the leaf, it is noted that the three

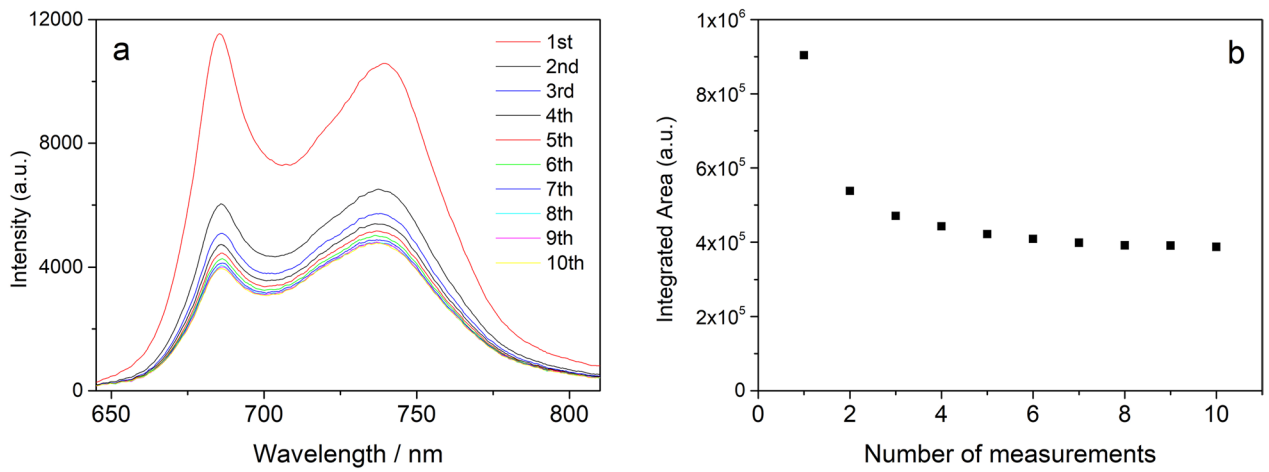

Fig. 4 **a** Ten replicate LED-IF measurements of a leaf sample acquired on the same spot and **b** integrated area defined under both fluorescence bands for each one of the 10 measurements. $\lambda_{exc} = 440$ nm

measurements were acquired on three different leaves. All spectra have been normalised with respect to the emission intensity at about 640 nm.

The fluorescence emission spectra obtained from the leaf are shown in Fig. 5 and as expected, two main bands are visible, at 685 nm and 735 nm, both attributed to chlorophyll species [12]. It is observed that the band at 685 nm exhibits its highest intensity for λ_{exc} at 475 and 500 nm. The highest intensity for the band at 735 nm, appears with λ_{exc} in the range of 500–575 nm. Clearly, the two fluorescence bands behave differently upon excitation of the leaf at different wavelengths and this is evident by observing the variation in the values of the ratio of their intensities at the maxima of the emission bands, I_{685}/I_{735}, as a function of λ_{exc} (Fig. 5b).

This sort of behaviour has been reported previously and is attributed to re-absorption of the emitted chlorophyll fluorescence at 685 nm by the chlorophyll absorption band at around 670 nm [48]. The green leaf pigments, chlorophylls and carotenoids, have broad absorption bands between 400 and 500 nm, so when the excitation wavelength is at that range, light does not penetrate deeply into the leaf tissue, thus chlorophyll fluorescence is mainly emitted from cells close to the leaf surface, and only little re-absorption takes place. With excitation light between 500 and 600 nm, that is not absorbed by carotenoids and penetrates more deeply into the green leaf mesophyll, the chlorophyll fluorescence is also emitted from the interior layers of the leaf and along its path to the surface, it likely suffers significant re-absorption compared to chlorophyll fluorescence induced by blue light excitation [48]. Although there exist differences on the biological characteristics between the leaf and the microorganisms investigated in the present study, the chlorophyll fluorescence is expected to show similar behaviour. This behaviour should be taken into account when interpreting fluorescence spectra of this type of samples, since factors such as the excitation wavelength, could affect the observed bands intensity and the relative intensity between bands. Moreover, a variability in intensity and intensity ratio is observed among different leaves or even on the same leaf if different areas are probed (the relative standard deviation of the band intensity at its spectral maximum for the three measurements can be as high as 50%; data not shown here). Especially for the intensity ratio I_{685}/I_{735}, this varies also depending on the content of the chlorophyll species [49], which should also be considered, while studying the fluorescence of such materials.

Figure 6 shows the fluorescence emission spectra collected from object A (see image in Fig. 1). The main band observed appears having its maximum at about 675 nm and reaches its highest intensity for $\lambda_{exc} = 425$ nm. The emission intensity is quite low upon excitation across the whole range of λ_{exc}; especially for $\lambda_{exc} = 575$ nm and $\lambda_{exc} = 600$ nm the band is hardly noticeable over the spectral background (spectra omitted from the graph). Observation of the fluorescence band at 675 nm is an indication that the biodeteriogen contains chlorophyll, confirming the findings of the classical taxonomy. The observed shift of the band emission maximum, compared to that of the leaf chlorophyll, is probably due to the reduced chlorophyll content of the biodeteriogen, which causes a shift of the chlorophyll fluorescence maximum to lower wavelengths [48, 50].

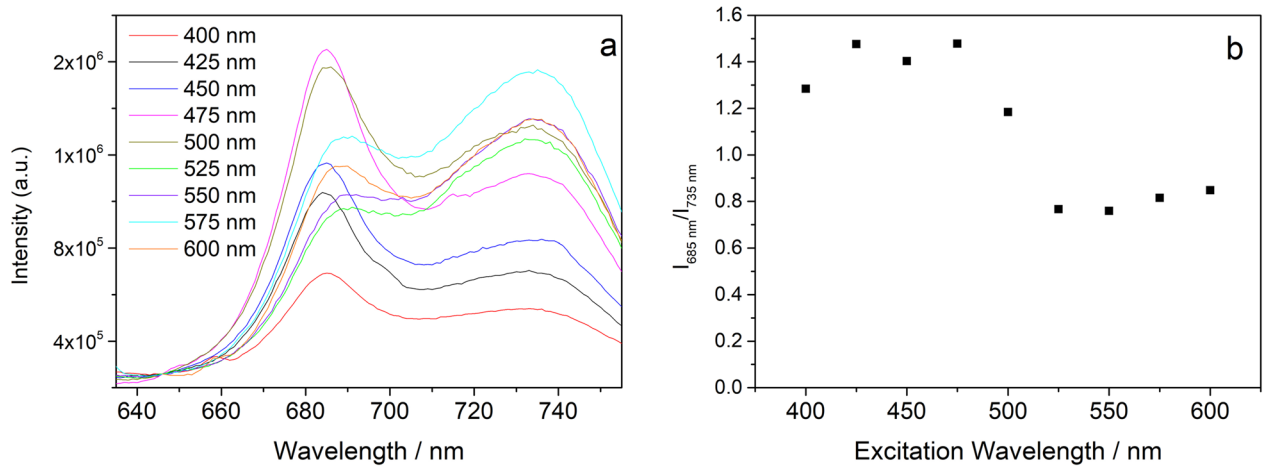

Fig. 5 **a** Fluorescence emission spectra of leaf samples collected upon excitation at various wavelengths in the range 400–600 nm and **b** Intensity ratio of the two main chlorophyll emission bands, I_{685}/I_{735}, as a function of excitation wavelength. Spectra were collected on the Fluoromax-P spectrometer

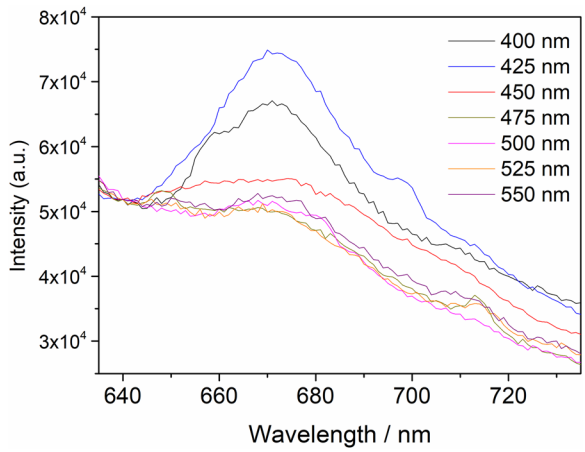

Fig. 6 Fluorescence emission spectra of object A at various excitation wavelengths in the range of 400–550 nm. Spectra were collected on the Fluoromax-P spectrometer

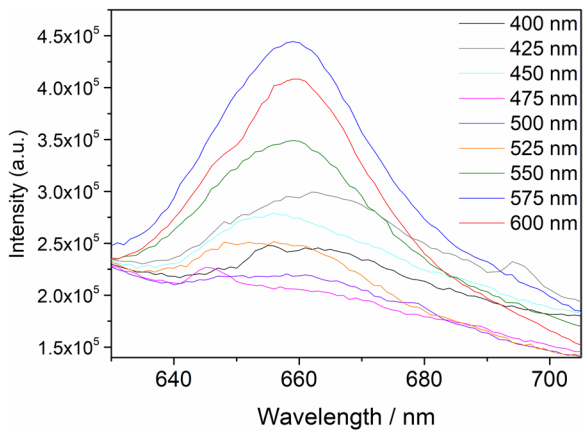

Fig. 7 Fluorescence emission spectra from object B at various excitation wavelengths in the range of 400–600 nm. Spectra were collected on the Fluoromax-P spectrometer

In the case of Object A, the excitation wavelength that leads to maximum fluorescence emission is $\lambda_{exc} = 425$ nm, a value close to the main absorption band of chlorophyll at 418 nm (Soret band), and this is also indicative of the presence of chlorophyll in this type of biodeterioration [19, 20]. The results obtained from object D are similar to the ones acquired for object A, therefore it was not deemed necessary to present them here.

Concerning object B, the fluorescence emission spectra are displayed in Fig. 7 (see also image in Fig. 1). The main emission band is observed to have its maximum at around 660 nm while the highest intensity is obtained at $\lambda_{exc} = 575$ nm. This observation suggests that the fluorophores in this biological crust are different compared to the ones on object A. Based on literature data, a potential chromophore is allophycocyanin that indeed fluoresces at 660 nm (see Table 1) [12]. Moreover, the fact that, for object B, the maximum intensity of fluorescence signal is observed at $\lambda_{exc} = 575$–600 nm could be correlated with the presence of cyanobacteria, which have an absorption maximum at about 570–650 nm (see Table 1) and this is actually in accordance with the classical taxonomy findings.

Based on these experimental results, it is apparent that there exist different fluorophores (biodeteriogens) on object B and objects A and D, given that their fluorescence bands appear in different wavelengths and the maximum fluorescence emission intensity is induced by different excitation wavelengths. These observations are in agreement with the results from the classical taxonomy analysis.

The effect of wetting the samples surface on the fluorescence signal

The surface of each sample has been wetted prior to analysis, as mentioned in "Experimental setup—materials and methods" Section, and two are the main reasons for this practice. First, it was observed in some preliminary experiments conducted in our laboratory that wetting the surface leads to an increase of the chlorophyll fluorescence intensity. This effect is not fully explained yet but there are two phenomena that could act synergistically. On the one hand, the application of water changes the optical properties of the sample surface, effectively the refractive index, reducing scattering and permitting incident light (here the LED light) to penetrate more efficiently in the rough biological surface thus resulting in higher fluorescence emission. On the other hand, photoautotroph microorganisms such as cyanobacteria are known to be able to resume their photosynthetic activity rapidly upon rehydration (called activation), which entails a 'greening' of the surface, obvious in our experiments soon after surface wetting, and a subsequent increase in fluorescence signal even within minutes [49]. It should be noted though that not all biodeteriogens are affected similarly by the presence of water. For example, fungi can survive in extreme environmental conditions, so the addition of water is not expected to affect their behaviour and subsequently their fluorescence signal. In order to further investigate this phenomenon, digital microscope images were acquired for the dry and wet surface of objects B and D (Fig. 8); a clear difference is noticed between the two surfaces, with the wet surface appearing greener.

The second reason for wetting the samples relates to an attempt to simulate a real case scenario. Meteorological phenomena, such as rainfall, snowfall, ice formation,

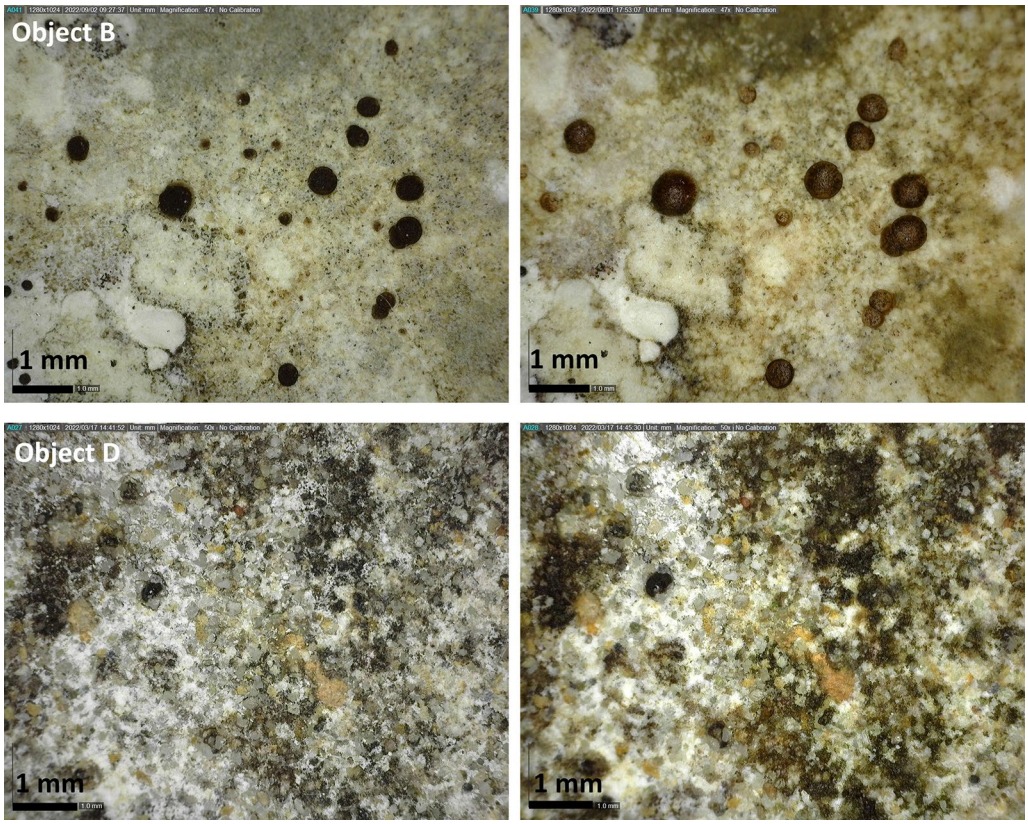

Fig. 8 Digital microscope images of objects B and D with their surface dry (left column) and wet (right column)

morning dew etc. affect the exterior of buildings and monuments as well as sculpture displayed outdoors by increasing the humidity on their surface. In order to better study the effect of humidity and water on the fluorescence signal of the biological materials investigated in this work, the samples were analysed both in their original state, i.e. dry, as well as wet following the procedure described in "Experimental setup—materials and methods" Section.

In this section, the effect of wetting of the biofilms on their fluorescence emissions is detailed. As a control, it was deemed necessary to acquire first the fluorescence signal from the substrate of each archaeological object, namely an area on its surface, where no sign of biological growth is detected under visual observation with a microscope. The objects were analysed on their back side, where the bulk material was observed, and LED-IF spectra were collected with $\lambda_{exc} = 375$ nm (Fig. 9). A broad emission band in the range of 500–600 nm is observed for most of the substrates with a varying intensity. This broad band has been reported in the literature and its origin is interpreted as emission from minerals, such as calcite (the main mineral in the objects of the present study), which is caused by adsorbed cations and

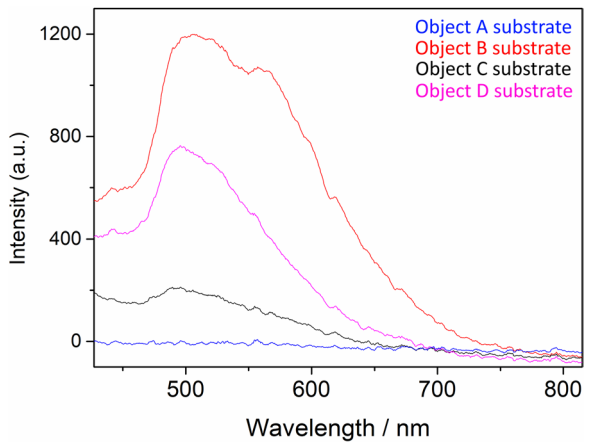

Fig. 9 Fluorescence emission spectra collected from the substrates of all four objects investigated (object A—blue, B—red, C—black and D—pink line), collected with the LED-IF instrument. $\lambda_{exc} = 375$ nm

by defects in the mineralogical periodicity [30, 51, 52]. It is worth noticing that the substrates are quite heterogeneous, fact that is reflected in the varying intensity of this band across the surface of the same object but, in

any case, the substrate spectra can serve as a background against which the biological material fluorescence spectra are compared.

Following acquisition of the substrate spectra, the biofilms (both in dry and wet state) for each one of the four objects were examined. In Fig. 10, the fluorescence emission spectra from two of the objects, A (Fig. 10a) and C (Fig. 10b), analysed with the ultraviolet LED source are depicted, with a spectrum of the *Hibiscus* leaf superimposed (green-coloured spectrum) serving as a reference for chlorophyll emission. As expected, a chlorophyll fluorescence band at around 680 nm was detected (Fig. 10a) and by comparing the spectra of the dry and wet samples, it is evident that upon wetting of the surface, the chlorophyll signal increases by a factor of nearly 3. To eliminate the possibility that this signal enhancement could happen also in non-biological material, the fluorescence spectra of the substrates, dry and following wetting, were recorded as well, and are shown in Fig. 10. The only signal observed for both the dry and the wet substrate is a low-intensity broad band emission at around 500 nm (as also seen in Fig. 9) which does not change in intensity at either the dry or the wet state. This implies that indeed, applying water on the sample surface leads to a noticeable increase in fluorescence emission within a few minutes, in the case of the biofilm, while it does not affect significantly the fluorescence signal from the substrate.

It is noteworthy that the band at 500 nm, although originating from the substrate shows lower intensity for the bare substrate than for the biofilm. This could be explained on the basis of a number of reasons. First, the biodeteriorated surface morphology and structure has been altered by the microorganisms colonising it, which may have changed the crystal structure of the substrate inducing defects and altering its intrinsic fluorescence signal. Second, the substrates have a quite heterogeneous macroscopic structure; even analysis at different points on the same object results in fluorescence intensity variations. Also, it is likely that the biodeteriorated surface presents other impurities apart from microorganisms (such as environmental pollution deposits) that may be responsible for additional background emissions. So, in reality, it is not possible to compare quantitatively, namely in terms of their fluorescence emission intensity, the substrate/bulk material to the biofilm, since the two surfaces are very different in nature. The analysis of the substrate can only give qualitative information as for the origin of specific bands.

For all samples analysed, a similar behaviour was observed; the chlorophyll signal was consistently higher on a wetted surface. In some cases, wetting of the sample even made possible the detection of distinct spectral features (see where arrow points in Fig. 10b), which were hardly noticeable in the dry sample spectra. These observations clearly point out to an important climatic parameter that needs to be considered when analysing biodeteriogens on monuments, and this relates to weather conditions and seasonality. If the season is characterised by reduced humidity, i.e. summer, some biodeteriogens that contain chlorophyll might not be detected or their quantity could be underestimated leading to wrong conclusions about the presence and extent of biological growth on a monument. A humid or rainy season would be preferred when photoautotroph organisms need to be detected in-situ by means of their fluorescence.

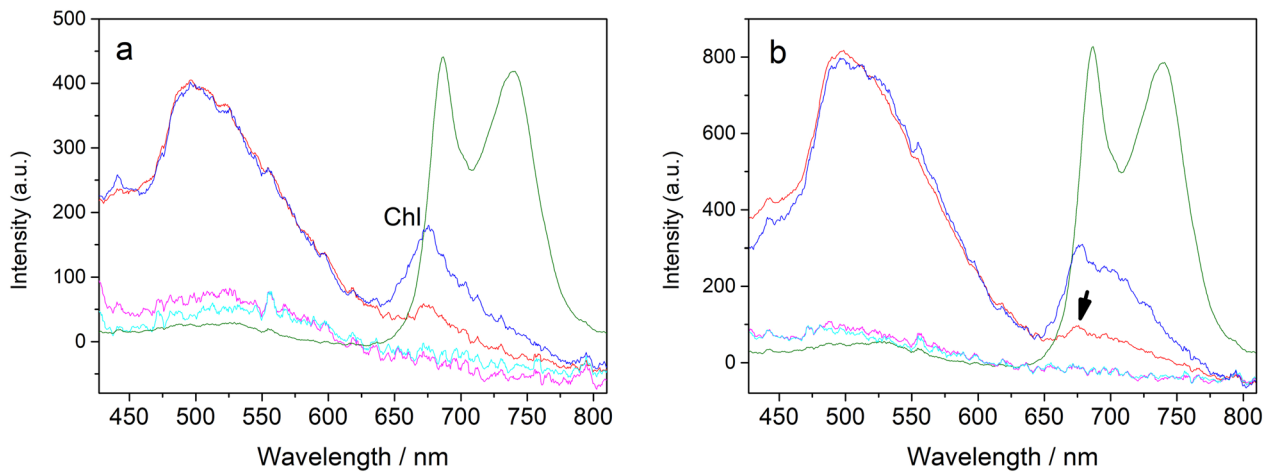

Fig. 10 Fluorescence emission spectra of object A (**a**) and C (**b**) collected with the LED-IF instrument, $\lambda_{exc} = 375$ nm. Dry sample (red), wet sample (blue), leaf (green), dry substrate (pink) and wet substrate (cyan)

In the context of this study and given that our main objective was the investigation of the capabilities and limitations of the LED-IF instrument and the analysis methodology, it was decided that all the samples be wetted prior to analysis, in order to ensure that the photoautotroph biodeteriogens, if present, will be more easily detected.

Comparison of the two LED excitation sources

The experimental findings concerning the fluorescence properties of the biodeteriogens ("Fluorescence characteristics of biodeteriogens" Section) showed that objects A and D, as well as the leaf, exhibit maximum fluorescence signal with excitation wavelengths in the range of 425–475 nm. Based on the LED sources available in the market, it was decided to use a diode emitting in the range of 400–450 nm.

It should be noted here, that sample B exhibited maximum fluorescence signal intensity for excitation wavelengths over 550 nm due to the different fluorophores present in this sample (i.e. cyanobacteria) (see also "Fluorescence characteristics of biodeteriogens" Section). It was decided though not to select a LED source emitting near 550 nm, because this way chlorophyll species would not be efficiently excited and furthermore because such a choice would eliminate the possibility to record potential emission bands from other fluorophores below 550 nm. Therefore, in the present study, two LEDs were assessed based on their ability to excite the fluorophores present in the biodeteriogens: one emitting in the ultraviolet (UV), $\lambda_{exc} = 375$ nm, and another in the visible (Vis, blue), $\lambda_{exc} = 440$ nm.

As a test, the *Hibiscus* leaf was analysed with both LEDs to study the effect of different excitation wavelengths and power on the induced fluorescence and spectral data are shown in Fig. 11 (with no spectral pre-processing). With either excitation source the fluorescence emission bands of chlorophyll species in the leaf are clearly evident. Comparing the emission spectra of the leaf obtained with both LEDs delivering approximately the same power (P = 6 mW) on the sample surface, it is evident that visible excitation yields a clean spectrum with a higher value of signal-to-noise ratio (SNR = 43), compared to UV excitation (SNR = 25). The noise was calculated as the standard deviation of a baseline spectrum. It should be noted, however, that measurements were not acquired on the same spot of the leaf, so some deviations are expected in the intensity. Nevertheless, the blue LED source yielded consistently spectra with higher SNR values. By increasing the power of the visible LED, from P = 6 mW to P = 26 mW the intensity of the chlorophyll emission at 685 nm increased approximately by a factor of 4, following almost linearly the increase of the source power.

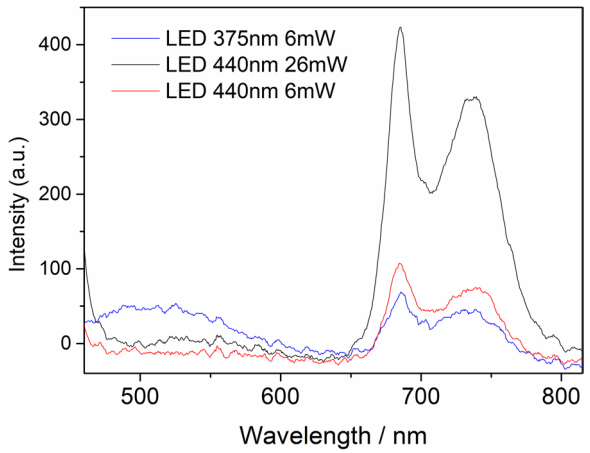

Fig. 11 Fluorescence emission spectra of a leaf sample acquired with the LED-IF instrument. $\lambda_{exc} = 440$ nm with P = 26 mW (black) and P = 6 mW (red). $\lambda_{exc} = 375$ nm with P = 6 mW (blue)

Discrimination of different types of biodeterioration

The major goal of this study has been to investigate whether the new portable LED-IF instrument is capable of detecting and discriminating the possible types of biodeterioration products that are present on monuments on the basis of their fluorescence profile. Figure 12 depicts fluorescence emission spectra from each one of the archaeological objects, collected with both LEDs operating at their maximum available power. The spectra have been normalised with respect to the intensity of the emission band at around 500 nm.

Object A exhibits a main emission band at 675 nm and a shoulder around 720 nm, both attributed to chlorophyll species. The spectra are similar to those acquired on the spectrofluorometer (see Fig. 6). The reason for the overall different spectral profile and the shift of the bands in comparison to the observed leaf spectra is explained in "Fluorescence characteristics of biodeteriogens" Section.

A comparison of the spectra in terms of SNR shows that the visible LED at 440 nm gives rise to cleaner spectra and this is attributed to its higher power output. It is, however, understood that other factors are critical as well, for example, the overall absorbance of the biofilm at the excitation wavelength.

The analysis of objects B and C was performed on the dark round spots (see Fig. 1) but since the area probed with the portable LED-IF instrument is larger, about 2×2 mm^2, recording of emissions from the surrounding area cannot strictly be avoided. On object B, a predominant fluorescence band at 660 nm was detected, along with chlorophyll bands of lower intensity at about 675 and 720 nm. The band at 660 nm originates most probably from allophycocyanin (APhC), present in

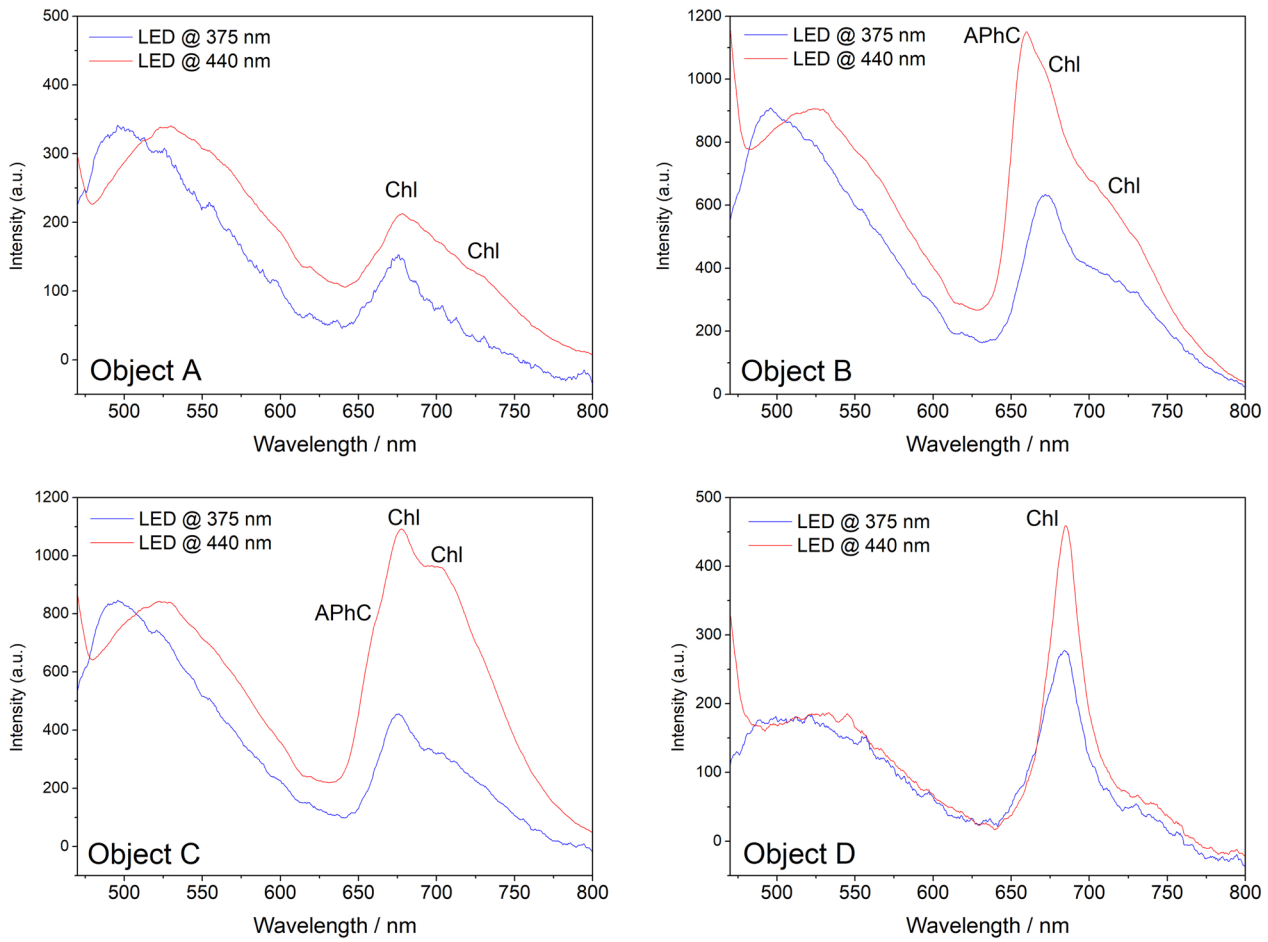

Fig. 12 Fluorescence emission spectra of the four objects, acquired with excitation by the two LEDs, $\lambda_{exc} = 375$ nm (blue line) and $\lambda_{exc} = 440$ nm (red line) with the maximum available power from either source

cyanobacteria, and this behaviour is in accordance with the fluorescence emission spectra acquired with the spectrofluorometer (see Fig. 7).

Fluorescence emission spectra, collected from object C, revealed the presence of chlorophyll bands at 678 and 720 nm, as well as a shoulder at 660 nm, observed better with visible excitation. This finding indicates that object C contains both chlorophyll and allophycocyanin with the former prevailing against the latter. Finally, after analysis of object D, a band appears at 685 along with a shoulder at 735 nm, which are both attributed to chlorophyll species and the fluorescence emission maxima coincide with those recorded on the leaf.

The fluorescence analysis results, obtained by use of the LED-IF probe, are in agreement with the classical taxonomy analysis. In objects B and C, fluorescence analysis revealed the presence of (a) allophycocyanin, which is a pigment characteristic of cyanobacteria that are contained in lichens and (b) chlorophyll, which is also contained in cyanobacteria. In objects A and D, fluorescence shows mainly the presence of chlorophyll, which is the main pigment for algae. It is worth noting that although based on the classical taxonomy, fungi were present in some samples, no relevant fluorescence signal was recorded. This can be explained by the fact that the fluorophores existing in fungi exhibit absorption and fluorescence maxima in the UV range. There are some fluorescence bands in the visible but these might be overlapping with the fluorescence coming from the substrate, which lies in the same spectral area (See Table 1 and references therein).

These four objects illustrate clearly different cases of biodeterioration. In object D, chlorophyll is detected with the emission band maxima appearing at the same wavelengths as those in the leaf emissions. In object A, chlorophyll emission was also detected but with a band shift compared to the leaf chlorophyll emission. In object B,

the signal originates mainly from allophycocyanin with a small contribution from chlorophyll. Finally, in object C, chlorophyll emission bands prevail over the one from allophycocyanin. These results indicate that with the present portable LED-IF spectrometer, it is possible to detect different types of biodeteriogens that could (co-) exist on monument surfaces, opening new possibilities in the protection of heritage artefacts, historic buldings and monuments against biodeterioration.

It is finally noted that, in the context of the present study, major colonizers were identified to group level (black microcolonial fungi, eukaryotic algae and lichens) based on their morphological features available at the time of their study. Further characterization, within each group, down to family or genus level requires the presence of different diagnostic fluorophores and is currently a subject under investigation.

Conclusions

The present study has shown that LED-Induced Fluorescence spectroscopic analysis, conducted with a portable, compact and low-budget instrument, has the capacity to provide information that facilitates detection of and discriminating among several types of biodeterioration products, such as algae and cyanobacteria. An evaluation of the LED-IF instrument has been performed as regards key optical components, such as the LED sources, measurement parameters and sample preparation procedures, which led to the development of a straightforward methodology suitable for the successful characterization and assessment of the biodeteriogens. From the results presented herein, it is evident that wetting of the object surface prior to analysis leads to activation of the existing, mainly photoautotroph, organisms, and in turn to a more sensitive detection of these organisms on the basis of their fluorescence emission signal. As regards the appropriate LED source that would excite successfully the fluorophores in the biofilms, a diode emitting in the range of 375–440 nm with a power of a few mW is considered a reasonable choice that can excite most fluorophores contained in biodeteriogens, which are commonly encountered in monuments exposed to Mediterranean climate conditions. The instrument is expected to be soon tested on site on different monuments and biodeteriogen cases. The authors are confident that this equipment will offer conservators, heritage scientists and other professionals a quick, safe and reliable tool for the detection of different types of biodeterioration and will help them make informed decisions concerning proper treatment and protection of historic buildings, monuments and artefacts.

Abbreviations

LED-IF: Light Emitting Diode-Induced Fluorescence; PSI: Photosystem I; PSII: Photosystem II; NADPH: Reduced Nicotinamide Adenine Dinucleotide; λ_{abs}: Wavelength of absorption bands; λ_{em}: Wavelength of fluorescence emission bands; LIF-LIDAR: Laser Induced Fluorescence–Light Detection and Ranging; FWHM: Full Width at Half Maximum; Chl: Chlorophyll; λ_{exc}: Excitation wavelength; P: Power; APhC: Allophycocyanin; SNR: Signal-to-noise ratio.

Acknowledgements

The authors would like to gratefully acknowledge the conservators of Lithou Syntirisis Ltd. (Athens, Greece) for insightful discussions on biodeterioration of monuments and Prof. Kiriakos Kotzampasis (Department of Biology, University of Crete) for fruitful discussions about chlorophyll. The authors also would like to thank the members of the PhoHS group at IESL-FORTH: Kristalia Melessanaki for helping with the treatment of the samples, especially the wetting procedure, Konstantinos Hatzigiannakis for valuable advice on fluorescence and Dr. Victor Piñon for reviewing the manuscript and formatting the figures.

Author contributions

AG performed all the analyses, interpretation of the data and was the major contributor in writing the manuscript. AP has helped with the data acquisition and interpretation. PS has developed the hardware of the LED-IF instrument used in the present study. IP has contributed in preparing the biological samples and performed the classical taxonomy. DA made substantial contributions to the conception of the work, the interpretation of data and in revising the manuscript. PP made substantial contributions to the conception and design of the work. All authors read and approved the final manuscript.

Funding

Financial support for this work has been provided through project CALLOS: *Conservation of Athens antiquities with Laser and Lidar technologies Open to Science and public* (MIS-5056208), in the context of the "Open Innovation in Culture" action co-funded by the European Regional Development Fund (ERDF) and national resources through the Operational Program "Competitiveness, Entrepreneurship & Innovation" (NSRF-EPAnEK, 2014-20, Greece). AP was also supported through project SpArch: *Spectrochemical Analysis of Archaeological Bio-Organic Residues* (HFRI-FM17-3542), funded by the Hellenic Foundation for Research and Innovation, Greece.

Availability of data and materials

The datasets used and/or analysed during the current study are available from the corresponding author on reasonable request.

Declarations

Competing interests

The authors declare no competing interests.

Author details

[1]Institute of Electronic Structure and Laser, Foundation for Research and Technology-Hellas (IESL-FORTH), 100 N. Plastira St., 70013 Heraklion, Crete, Greece. [2]Section of Ecology and Systematics, Department of Biology, School of Science, National and Kapodistrian University of Athens, Panepistimioupoli, 15784 Athens, Greece. [3]Department of Chemistry, University of Crete, 71003 Heraklion, Crete, Greece.

Received: 2 June 2022 Accepted: 9 November 2022
Published online: 29 December 2022

References

1. Macedo MF, Miller AZ, Dionısio A, Saiz-Jimenez C. Biodiversity of cyanobacteria and green algae on monuments in the Mediterranean Basin: an overview. Microbiology. 2009;155:3476–90.

2. Scheerer S, Ortega-Morales O, Gaylarde C. Microbial deterioration of stone monuments—an updated overview. Adv Appl Microbiol. 2009. https://doi.org/10.1016/S0065-2164(08)00805-8.
3. Bhatnagar P, Khan AA, Jain SK, Rai MK. Biodeterioration of Archaeological Monuments and Approach for Restoration. In: Jain SK, Khan AA, Rai MK, editors. Geomicrobiology. Boca Raton: CRC Press; 2010. p. 255–302.
4. Dakal TC, Cameotra SS. Microbially induced deterioration of architectural heritages: routes and mechanisms involved. Envir Sci Europe. 2012;24(36):1–13.
5. Li Q, Zhang B, Yang X, Ge Q. Deterioration-associated microbiome of stone monuments: structure, variation, and assembly. Appl Environ Microb. 2018;84(1–19):e02680-e2717.
6. Santo AP, Cuzman OA, Petrocchi D, Pinna D, Salvatici T, Perito B. Black on white: microbial growth darkens the external marble of florence cathedral. Appl Sci. 2021;11(1–17):6163.
7. Mihajlovski A, Seyer D, Benamara H, Bousta F, Di Martino P. An overview of techniques for the characterization and quantification of microbial colonization on stone monuments. Ann Microbiology. 2015;65:1243–55.
8. Scheerer S. Microbial biodeterioration of outdoor stone monuments. Assessment methods and control strategies. PhD thesis, Cardiff University (2008)
9. Förster LS, Livingston R. The absolute quantum yields of the fluorescence of chlorophyll solutions. J Chem Phys. 1952;20:1315–20.
10. Walsh Yeh S, Ong LJ, Clark JH, Glazer AN. Fluorescence properties of allophycocyanin and a crosslinked allophycocyanin trimer. Cytometry. 1987;8:91–5.
11. https://omlc.org/spectra/PhotochemCAD/html/041.html. Beta-carotene (omlc.org). Last Accessed 11 Sep 2022
12. Franck F, Juneau P, Popovic R. Resolution of the Photosystem I and Photosystem II contributions to chlorophyll fluorescence of intact leaves at room temperature. Biochim Biophys Acta. 2002;1556:239–46.
13. Caerovic ZG, Samson G, Morales F, Tremblay N, Moya I. Ultraviolet-induced fluorescence for plant monitoring: present state and prospects. Agronomie. 1999;19:543–78.
14. Lamb JJ, Rokke G, Hohmann-Marriott MF. Chlorophyll fluorescence emission spectroscopy of oxygenic organisms at 77 K. Photosynthetica. 2018;56:105–24.
15. Raimondi V, Cecchi G, Longnoli D, Palombi L, Ballerini G. Fluorescence LIDAR Technique for Cultural Heritage. Last Accessed 11 Apr 2022 http://www.science4heritage.org/COSTG7/booklet/chapters/lidar.htm.
16. Ayudhya TIN, Posey FT, Tyus JC, Dingra NN. Using a microscale approach to rapidly separate and characterize three photosynthetic pigment species from fern. J Chem Educ. 2015;92:920–3.
17. Govindjee, Shevela D. Adventures with cyanobacteria: a personal perspective. Front Plant Sci. 2011. https://doi.org/10.3389/fpls.2011.00028.
18. Bergmann T, Beer S, Maeder U, Burg JM, Schlupp P, Schmidts T, Runkel F, Fiebich M. Development of a skin phantom of the epidermis and evaluation by using fluorescence techniques. In: Coté GL, Nordstrom RJ, editors. Optical Diagnostics and Sensing XI Toward Point-of-Care Diagnostics and Design and Performance Validation of Phantoms Used in Conjunction with Optical Measurement of Tissue III. Bellingham: SPIE; 2011.
19. Stockett MH, Musbat L, Kjær C, Houmøller J, Toker Y, Rubio A, Milne BF, Nielsen SB. The Soret absorption band of isolated chlorophyll a and b tagged with quaternary ammonium ions. Phys Chem Chem Phys. 2015;17:25793–8.
20. Rachma D, Sandiningtyas V, Suendo V. 2010 Isolation of Chlorophyll a from spinach and its modification using Fe^{2+} in photostability study. In: Proc Third Intern Conf Mathem Natural Sci. 859–73.
21. Averina SG, Velichko NV, Pinevich AA, Senatskaya EV, Pinevich AV. Non-a chlorophylls in cyanobacteria. Photosynthetica. 2019;57:1109–18.
22. Ustinova AO, Bratchenko IA, Artemyev DN. Monte Carlo simulation of skin multispectral. J of Biomed Photon Engin. 2019;5(1–6):020306.
23. Pohlker C, Huffman JA, Poschl U. Autofluorescence of atmospheric bioaerosols—fluorescent biomolecules and potential interferences. Atmos Meas Tech. 2012;5:37–71.
24. Zhang Y, Sukthankar P, Tomich JM, Conrad GW. Effect of the synthetic NC-1059 peptide on diffusion of riboflavin across an intact corneal epithelium. Invest Ophth Vis Sci. 2012;53:2620–9.
25. Kudo H, Sawai M, Wang X, Gessei T, Koshida T, Miyajima K, Saito H, Mitsubayashi K. A NADH-dependent fiber-optic biosensor for ethanol determination with a UV-LED excitation system. Sensors Actuat B. 2009;141:20–5.
26. Rabasovic MD, Pantelic DV, Jelenkovic BM, Curcic SB, Rabasovic MS, Vrbica MD, Lazovic VM, Curcic BPM, Krmpot AJ. Nonlinear microscopy of chitin and chitinous structures: a case study of two cave-dwelling insects. J Biomed Opt. 2015;20(1–10):016010.
27. Saari SE, Putkiranta MJ, Keskinen J. Fluorescence spectroscopy of atmospherically relevant bacterial and fungal spores and potential interferences. Atmos Environ. 2013;71:202–9.
28. Dalterio RA, Nelson WH, Britt D, Sperry J, Psaras D, Tanguay JF, Suib SL. Steady-state and decay characteristics of protein tryptophan fluorescence from bacteria. Appl Spectrosc. 1986;40:86–90.
29. Nevin A, Spoto G, Anglos D. Laser spectroscopies for elemental and molecular analysis in art and archaeology. Appl Phys A. 2012;106:339–61.
30. Raimondi V, Cecchi G, Pantani L, Chiari R. Fluorescence lidar monitoring of historic buildings. Appl Optics. 1998;37:1089–98.
31. Lognoli D, Lamenti G, Pantani L, Tirelli D, Tiano P, Tomaselli L. Detection and characterization of biodeteriogens on stone cultural heritage by fluorescence lidar. Appl Optics. 2002;41:1780–7.
32. Weibring P, Edner H, Svanberg S. Versatile mobile lidar system for environmental monitoring. Appl Optics. 2003;42:3583–94.
33. Weibring P, Johansson T, Edner H, Svanberg S, Sundner B, Raimondi V, Pantani L. Fluorescence lidar imaging of historical monuments. Appl Optics. 2001;40:6111–20.
34. Palombi L, Lognoli D, Raimondi V, Cecchi G, Hällström J, Barup K, Conti C, Grönlund R, Johansson A, Svanberg S. Hyperspectral fluorescence lidar imaging at the Colosseum, Rome: Elucidating past conservation interventions. Opt Express. 2008;16:6794–808.
35. Raimondi V, Cecchi G, Lognoli D, Palombi L, Gronlund R, Johansson A. The fluorescence lidar technique for the remote sensing of photoautotrophic biodeteriogens in the outdoor cultural heritage: A decade of in situ experiments. Int Biodeter Biodegr. 2009;63:823–35.
36. Wang X, Duan Z, Brydegaard M, Svanberg S, Zhao G. Drone-based area scanning of vegetation fluorescence height profiles using a miniaturized hyperspectral lidar system. Appl Phys B. 2018. https://doi.org/10.1007/s00340-018-7078-7.
37. Duan Z, Li Y, Wang J, Zhao G, Svanberg S. Aquatic environment monitoring using a drone-based fluorosensor. Appl Phys B. 2019. https://doi.org/10.1007/s00340-019-7215-y.
38. Mukunda DC, Joshi VK, Mahato KK. Light emitting diodes (LEDs) in fluorescence-based analytical applications: a review. Appl Spectrosc Rev. 2022;57:1–38.
39. Dong Y, Liu X, Mei L, Feng C, Yan C, He S. LED-induced fluorescence system for tea classification and quality assessment. J Food Eng. 2014;137:95–100.
40. Mustafic A, Li C, Haidekker M. Blue and UV LED-induced fluorescence in cotton foreign matter. J Biol Eng. 2014. https://doi.org/10.1186/1754-1611-8-29.
41. Gao F, Dong Y, Xiao W, Yin B, Yan C, He S. LED-induced fluorescence spectroscopy technique for apple freshness and quality detection. Postharvest Biol Tec. 2016;119:27–32.
42. Ding W, Gao F, Yan C. 2016 LED-induced Fluorescence Spectroscopy Technique for Milk Freshness Detection. 15th Intern Conf Optical Communic Netw (ICOCN) Hangzhou 1–3.
43. Campos AT, Quintella CM, Meira M, Luna S. Prediction of Sulfur content in diesel/biodiesel blends using LED-induced fluorescence associated with multivariate calibration. J Braz Chem Soc. 2018;29:1367–72.
44. Mounier A, Lazare S, Le Bourdon G, Aupetit C. LEDμSF: a new portable device for fragile artworks analyses application on medieval pigments. Microchem J. 2016;126:480–7.
45. Siozos P, Philippidis A, Anglos D. Portable laser-induced breakdown spectroscopy/diffuse reflectance hybrid spectrometer for analysis of inorganic pigments. Spectrochim Acta B. 2017;137:93–100.
46. Lakowicz JR. Principles of fluorescence spectroscopy. Berlin: Elsevier; 2006.
47. Maxwell K, Johnson GN. Chlorophyll fluorescence—a practical guide. J Exp Bot. 2000;51:659–68.
48. Buschmann C. Variability and application of the chlorophyll fluorescence emission ratio red/far-red of leaves. Photosynth Res. 2007;92:261–71.
49. Chennu A, Grinham A, Polerecky L, de Beer D, Al-Najjar MAA. Rapid reactivation of cyanobacterial photosynthesis and migration upon rehydration of dessicated marine microbial mats. Front Microbiol. 2015. https://doi.org/10.3389/fmicb.2015.01472.

50. Subhash N, Mohanan CN. Curve-fit analysis of chlorophyll fluorescence spectra: application to nutrient stress detection in sunflower. Remote Sens Environ. 1997;60:347–56.
51. Cecchi G, Pantani L, Raimondi V, Tirelli D. Fluorescence LIDAR Technique for the remote sensing of stony materials in ancient buildings. Proc SPIE. 1996;2960:163–71.
52. Toffolo MB, Ricci G, Caneve L, Kaplan-Ashiri I. Luminescence reveals variations in local structural order of calcium carbonate polymorphs formed by different mechanisms. Sci Rep. 2019;9:16170.

Publisher's Note